Oscillatory inertial focusing in infinite microchannels

Baris R. Mutlu[a], Jon F. Edd[a,b], and Mehmet Toner[a,c,1]

[a]BioMEMS Resource Center, Center for Engineering in Medicine and Surgical Services, Massachusetts General Hospital, Harvard Medical School, Boston, MA 02114; [b]Massachusetts General Hospital Cancer Center, Harvard Medical School, Boston, MA 02114; and [c]Shriners Hospitals for Children, Boston, MA 02114

Edited by David A. Weitz, Harvard University, Cambridge, MA, and approved June 15, 2018 (received for review December 21, 2017)

Inertial microfluidics (i.e., migration and focusing of particles in finite Reynolds number microchannel flows) is a passive, precise, and high-throughput method for microparticle manipulation and sorting. Therefore, it has been utilized in numerous biomedical applications including phenotypic cell screening, blood fractionation, and rare-cell isolation. Nonetheless, the applications of this technology have been limited to larger bioparticles such as blood cells, circulating tumor cells, and stem cells, because smaller particles require drastically longer channels for inertial focusing, which increases the pressure requirement and the footprint of the device to the extent that the system becomes unfeasible. Inertial manipulation of smaller bioparticles such as fungi, bacteria, viruses, and other pathogens or blood components such as platelets and exosomes is of significant interest. Here, we show that using oscillatory microfluidics, inertial focusing in practically "infinite channels" can be achieved, allowing for focusing of micron-scale (i.e. hundreds of nanometers) particles. This method enables manipulation of particles at extremely low particle Reynolds number (Re_p < 0.005) flows that are otherwise unattainable by steady-flow inertial microfluidics (which has been limited to $Re_p > \sim 10^{-1}$). Using this technique, we demonstrated that synthetic particles as small as 500 nm and a submicron bacterium, *Staphylococcus aureus*, can be inertially focused. Furthermore, we characterized the physics of inertial microfluidics in this newly enabled particle size and Re_p range using a Peclet-like dimensionless number (α). We experimentally observed that $\alpha >> 1$ is required to overcome diffusion and be able to inertially manipulate particles.

inertial microfluidics | oscillatory flow | bacteria focusing | Brownian motion | hydrodynamic lift

Inertial microfluidics—manipulation and focusing of particles in microchannels using inertial lift forces—has been employed in several key technologies since it was first demonstrated by Di Carlo et al. (1). First observed by Segré and Silberberg with millimeter-scale particles flowing through a large (~1 cm) circular tube (2), randomly distributed particles laterally migrate to equilibrium focus positions that are predetermined by the flow characteristics and the channel geometry. This inertial migration enables passive and precise manipulation of bioparticles in microchannels and has been utilized for aligning, ordering, or separating targeted cells in blood. This technology has been used in various biomedical applications, including phenotypic cell screening, blood fractionation, and rare-cell (e.g., circulating tumor cells, CTCs) isolation. Di Carlo et al. (3) used asymmetric curves to achieve differential inertial focusing for separation of larger blood cells (RBCs and WBCs) from platelets. Lee et al. (4) used a spiral geometry for size-based separation, based on cell cycle and DNA content. Later, a similar spiral design was used for isolation of CTCs from whole blood (5). Sollier et al. (6) employed sudden expansion channels in combination with Vortex technology to isolate CTCs from whole blood. Gossett et al. (7) developed a high-throughput cytometer to assay cell deformability and showed that it can be used to assess lymphocyte activation and stem cell differentiation. Ozkumur et al. (8) used inertial focusing in a multistage CTC isolation chip to align and order nucleated cells after on-chip debulking of blood, to facilitate magnetic separation of WBCs from CTCs. Martel et al. (9) developed a bioparticle concentrator, by repetitive focusing of particles and siphoning a small portion of the flow at each stage. Recently, 3D stacking of chips has been explored, which in return significantly improved the throughput of the devices (10, 11). Inertial microfluidics have also been used for sheathless alignment of cells for flow cytometry (12), size-based separation of WBCs from lysed blood (13), whole-blood fractionation (14), and several other applications as summarized in a review by Martel and Toner (15).

Despite the wide breadth of its applications, inertial microfluidics has been confined to particles that are a few microns or larger (i.e., not smaller than an RBC), because of the strong correlation between the inertial lift forces and the particle size. Smaller particles traveling in typical microchannels (having a cross-sectional dimension of tens of microns) require drastically longer channels for focusing (in the order of meters), increasing the pressure requirement and the footprint of the channel to the extent that the system becomes unfeasible. Inertial manipulation of smaller bioparticles such as fungi, bacteria and other pathogens, or blood components such as extracellular microvesicles is of significant interest. For instance, identifying the infecting agent in a timely manner is crucial for the treatment of septic patients (16). Furthermore, recent studies show that exosomes carry information regarding primary tumor and can help with cancer diagnostics (17, 18). However, thus far, applications of inertial microfluidics have been limited to large bioparticles (blood cells, CTCs, stem cells, etc.). While there are a few studies which report working with fluids that include small pathogens, they operate by manipulating the larger cells. For instance, Mach and Di Carlo (19) reported a blood filtration device, which inertially manipulates the RBCs while the bacteria simply follow the streamlines. Similarly, Warkiani et al. (20) reported a malaria

Significance

Inertial microfluidics is a widely used technology which enables label-free manipulation of particles in microchannels. However, this technology has been limited to bioparticles larger than RBCs, due to the strong correlation between the inertial lift forces and the particle size. This paper presents a method to extend the capabilities of inertial microfluidics to smaller bioparticles, of which a plethora of clinically relevant types exist in the human body. Therefore, this method can be integrated with microfluidic devices for inertial manipulation of bioparticles that have defied all prior attempts, enabling a variety of applications in clinical diagnosis including cytometry of micron-scale bioparticles, isolation and characterization of pathogens and extracellular microvesicles, or phenotyping of cancer or stem cells at physiological shear stresses.

Author contributions: B.R.M., J.F.E., and M.T. designed research; B.R.M. performed research; B.R.M., J.F.E., and M.T. analyzed data; and B.R.M., J.F.E., and M.T. wrote the paper.

Conflict of interest statement: The authors have submitted a patent application related to the presented work.

This article is a PNAS Direct Submission.

[1]To whom correspondence should be addressed. Email: mtoner@hms.harvard.edu.

This article contains supporting information online at www.pnas.org/lookup/suppl/doi:10.1073/pnas.1721420115/-/DCSupplemental.

Published online July 10, 2018.

detection chip, which works by manipulating the WBCs, while the parasites travel unaffected. Therefore, expanding the capabilities of inertial microfluidics to micrometer- to submicron-scale particles is an unmet need.

Here, we show that using oscillatory microfluidics inertial focusing in practically infinite channels can be achieved, allowing for particle focusing at the micrometer scale and even smaller. Unlike traditional steady-flow microfluidics, oscillatory microfluidics switches the direction of the flow at a high frequency. Due to the symmetry of the velocity field along the flow axis, the inertial lift forces acting on the particle preserve their directionality when the flow direction is switched (Fig. 1*A*). By exploiting this symmetry, the focusing length can be extended indefinitely, even though the channel itself has a short, fixed length. This method enables manipulation and focusing of small particles at extremely low particle Reynolds number ($Re_p << 0.1$) flows, which are otherwise unattainable by inertial microfluidics. In addition, shorter channel length decreases the input pressure, which is a practical limiting factor that can cause the device features to deform or break. Operation at extremely low Re_p regime also enables lower flow velocities in channels with larger cross-sections, which reduces the shear stress experienced by the particles in the channel, allowing cell focusing at physiological conditions.

We demonstrated that using oscillatory flow inertial focusing can be achieved at $Re_p < 0.005$, about 20 times lower than previously attained (15), using synthetic particles as small as 500 nm, and a submicron round-shaped bacterium, *Staphylococcus aureus*, with a nominal size of 0.8 μm. Investigating the physics of inertial microfluidics in this newly enabled particle size and Re_p range, we showed that for particle sizes below 2 μm the self-diffusion rate of particles becomes significant with respect to the inertial migration rate of the particles. We proposed a dimensionless number (α) similar to the Peclet number to quantify this limitation, and our experimental observations demonstrated that $\alpha >> 1$ is necessary for the diffusion rate of the particles to be negligible compared with their inertial migration.

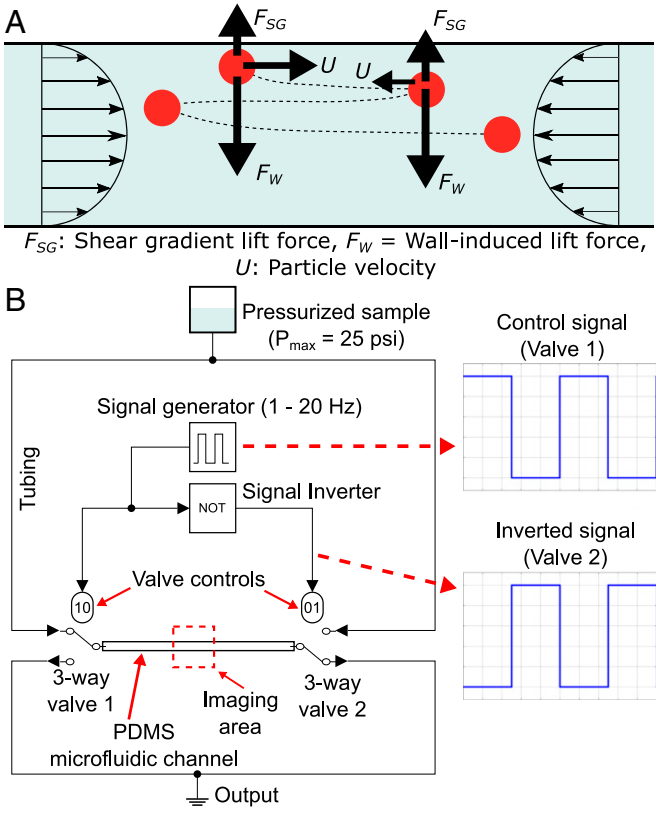

Fig. 1. Oscillatory inertial microfluidics theory and system design. (*A*) Inertial lift forces (F_W and F_{SG}) preserve their directionality when the velocity field is reversed, enabling indefinite extension of the inertial focus length. (*B*) Design schematic of the oscillatory microfluidics system used for inertial focusing.

Results and Discussion

Theoretical Background. Physics of inertial microfluidics, that is, the forces that cause the lateral migration and eventual focusing of particles in microchannels, are well-studied (21–25) (see *SI Appendix* for additional background). The major practical challenge for inertial microfluidics in very low Re_p flows is the extensive channel lengths required to attain focusing. To see this, consider first that the migration velocity of the particle due to inertial lift (U_P) can be calculated for a point particle as (assuming that the Stokes drag is balancing the inertial lift force) (1)

$$U_P = f_L \rho U_m{}^2 a^3 / 3\pi\mu H^2, \quad [1]$$

where f_L is a dimensionless lift coefficient, ρ is the density of the carrier fluid, U_m is the mean flow velocity in the channel, a is the particle diameter, μ is the viscosity of the carrier fluid, and H is the cross-sectional channel dimension of interest. Di Carlo (23) has calculated an estimated theoretical length which is required for inertial focusing, based on the U_P and the lateral migration length (of order H), for finite particles. Adapting the same method to point particles using Eq. **1**, a similar expression can be obtained for the required channel length for focusing (L_f) as

$$L_{f,theoretical} = \pi\mu H^3 / f_L \rho U_m a^3. \quad [2]$$

From this relationship, it is readily apparent that the required length is inversely correlated with U_m and a^3 (compared with U_m and a^2 for finite particles). Regardless of the point or finite particle assumption, the required length and the pressure requirement of the system increases drastically with decreasing Re_p, making it impractical (*SI Appendix*, Fig. S1).

Inertial Focusing in Oscillatory Flow. We demonstrated the inertial focusing of the particles in an oscillatory flow system by monitoring the particles over time at a fixed location in a straight microchannel. The system consists of a pressure source, a signal (pulse) generator, a valve-driving circuit, and two high-speed three-way valves (Fig. 1*B* and *SI Appendix*, Fig. S2). The valves are driven by two rectangular signals, where one of the signals is the inverse of the control signal so that the microfluidic circuit is completed in one direction or its reverse. The net flow in the microchannel is adjusted by the duty cycle of the control signal, where 50% corresponds to zero net flow, and any bias toward 0% or 100% duty cycle corresponds to a net flow in either direction. In our experiments, since we were monitoring the inertial migration of the same set of particles at a fixed location in the microchannel, we operated the system at zero net flow to be able to measure the focusing time of the particles.

Using the system, we were able to track an individual particle as it inertially migrates toward the center of the channel (see *Materials and Methods* for details) while oscillating (i.e. leaving and reentering the field of view; see Movie S1). However, for characterization of the inertial focusing behavior, we used fluorescence streak imaging with a group of particles (Fig. 2*A*). The focus time (t_f)—the time when inertial focusing was achieved—was evaluated using FWHM analysis using the streak images (Fig. 2*B*). Specifically, t_f was determined as the time point where FWHM reached its stable minimum. In this specific case (Fig. 2*B*), the focus time (t_f) and length (L_f) were determined as 48 s and 5.7 m, respectively, corresponding to two orders of magnitude enhancement to the physical channel length (~0.04 m). Note that experimental determination of L_f in an oscillatory flow requires measurement of particles' travel length. For streak

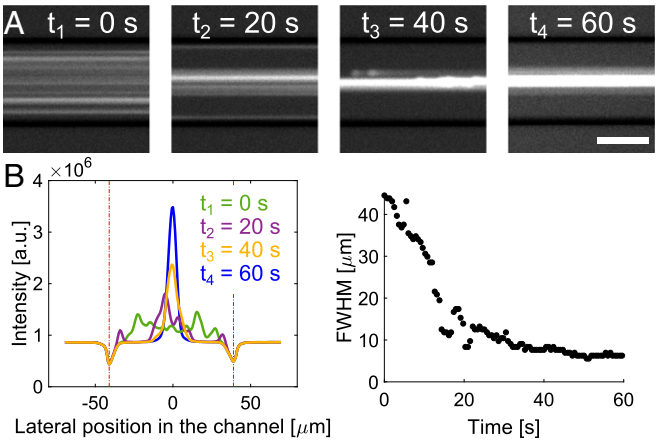

Fig. 2. Inertial focusing of particles using oscillatory microfluidics. (*A*) Streak images of oscillating 3.1-μm particles at the same position in the microfluidic device (H = 80 μm) over time. (Scale bar, 50 μm). (*B*) Intensity profile of the oscillating particles as they become focused and FWHM analysis over time, used for determining the focus time.

imaging, this requires very dilute particle solutions and the oscillatory travel path of the particles to be restricted to the imaged area of the microchannel, which is impractical at low oscillation frequencies. Due to these complications, we opted to calculate L_f based on the mean flow velocity using $L_f = t_f U_m$, where t_f is the experimentally determined focus time.

Upon validation of the oscillatory inertial focusing, the system was further tested with 3.1-, 4.8-, and 10-μm particles at varying flow velocities. The flow velocity in the microchannel was adjusted by varying the driving pressure from 1 psi to 25 psi. To keep the Re_p within a comparable range for different-sized particles, the tested pressure range was decreased as the particle size increased. This also ensured that when the particles were introduced to the channel there was no inertial focusing and particles were randomly distributed. The investigated frequency range for each particle size/pressure pair was selected based on the calculated mean velocity of the particles at a given pressure (P), focusing time (t_f) of the particles, and the response time of the microfluidic valves. Specifically, the minimum frequency was set to ensure that the particles stayed in the channel during their oscillatory travel. Thus, for instance, at high pressures (i.e., high U_m), lower frequencies were not tested as the particles would have to leave the channel. The maximum frequency (f = 20 Hz) was set to ensure that the response time of the valve (~5 ms) was small compared with the period of oscillation.

A trend between increased Re_p and decreased focus time (t_f) and focus length (L_f) was observed, for a constant particle size (Fig. 3). The fastest focusing (~5 s) was achieved with 10-μm particles at 5 psi driving pressure (Re_p = 0.083), while the slowest focusing (~10 min) was achieved with 3.1-μm particles at the same pressure (Re_p = 0.0068). Note that while faster focusing could be attained for 10-μm particles using a higher pressure, we opted to limit the pressure to maintain the Re_p values comparable to the smaller particles and ensure that the particles were not focused while entering the channel, as previously discussed. Thus, 5 psi was the highest pressure selected for 10-μm particles and the lowest pressure selected for 3.1-μm particles. Attained focus lengths (L_f) ranged approximately from 0.1 m up to 20 m (Fig. 3). The shortest L_f was achieved with the 10-μm particles at 5 psi, while the longest L_f was achieved with the smallest (3.1-μm) particles at 5 psi. For different-sized particles operating at a similar Re_p, L_f decreased with increasing a, which shows that a and L_f were explicitly correlated, beyond their implicit correlation via Re_p. For these sets of experiments, the channel width (the dimension that the migration is observed, H) was 80 μm, and thus a/H changed from 0.8 to 0.04 as the particle size got smaller. Therefore, we also concluded that the finite particle assumption did not hold for the explored particle size range.

We observed that the oscillation frequency affected the focusing behavior of the particles in our system. Increasing the oscillation frequency at a given Re_p resulted in slightly longer focus times (t_f) and focus lengths (L_f) (*SI Appendix*, Fig. S3). This result could be due to a combined effect of the system compliance [e.g. compliance of the polydimethylsiloxane (PDMS) and the tubing that connects the valves to the microfluidic chip] and the response time of the high-speed valves, which can delay the pressurization of the channels. We also observed an increased variance of the focusing time with increased oscillation frequency. We hypothesize that this phenomenon is due to the dynamic components (i.e., valves) of the system. Especially when operated at higher frequencies, we observed that the valves heat up, which could affect their dynamic response based on the duration of the operation and the temperature. We propose that the robustness of the system response can be improved by replacing the existing valves with higher-frequency

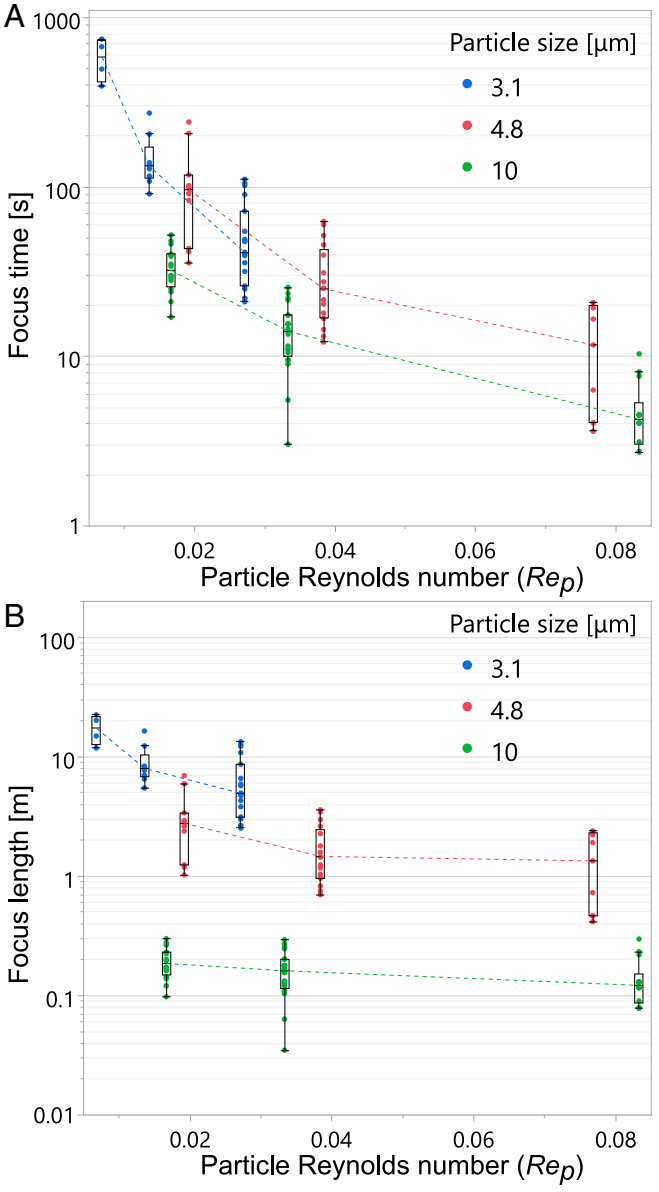

Fig. 3. Attained focus times (*A*) and focus lengths (*B*) of 3.1- to 10-μm particles at varying Re_p.

flow-control components (e.g., piezo valves), which would also enable operation at a higher frequency and shorter channel lengths.

Diffusion Limitation to Inertial Focusing for Micrometer-Scale Particles. A previously unexplored diffusion barrier on inertial focusing became evident when focusing particles that are 2 μm or smaller. We observed no focusing behavior with the 2-μm particles at the lowest tested pressure ($Re_p = 0.0025$), even after the particles had traveled for extremely long times and distances in the microchannel (10 min and 12.7 m, respectively) (Fig. 4*A*). Therefore, we concluded that at this critically low Re_p range a diffusion-limited no-inertial-focusing region was present. When the Re_p was increased to 0.0050, focusing was observed but the focus stream was uncharacteristically wide, as the system transitioned from diffusion-dominated to inertially controlled regime. Only when the Re_p was increased beyond 0.0075 was a typical, narrowly focused particle stream observed (Movie S2). Using the same device with 1-μm particles, focusing was observed only at the highest allowable pressure ($Re_p = 0.0031$). The different regimes based on the focus quality (i.e., width of the attained particle stream) were also quantified using FWHM evolution plots (Fig. 4*B*).

In the diffusion-limited particle-size range, higher flow velocities are required to improve Re_p and focus quality, while maintaining the inertial focusing length in the order of meters. This is impractical with steady flow due to the extreme pressure requirement, but oscillatory microfluidics allows virtually infinite lengths without increasing the pressure, and the minimum physical channel length is only limited by the maximum frequency of the high-speed valves. We used a shorter and wider device to focus *S. aureus* to compensate for the decrease in the Re_p due to the smaller particle size (0.8 μm), thereby enabling operation at a higher Re_p (0.0047) than 1-μm particles without increasing the pressure. Note that in this case the channel dimension in which we observed particle migration and focusing was two orders of magnitude larger than the particle size ($a/H = 0.01$). Under these parameters, we observed inertial focusing of bacteria (Fig. 4*C* and Movie S3), and the focus quality was similar to the previous results at a comparable Re_p range (*SI Appendix*, Fig. S4). For this set of experiments, the longest focus length ($L_f = 24.7 \pm 7.4$ m) was attained with 1-μm particles (Fig. 4*D*).

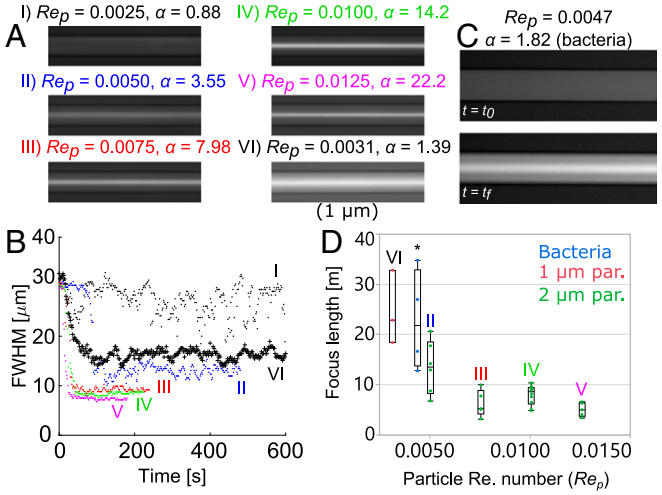

Fig. 4. Oscillatory inertial focusing with diffusion limitation. (*A*) Images of the microchannel ($L = 6.2$ cm, $H = 40$ μm) with the focused 2-μm (and 1-μm) particles after t_f and their corresponding Re_p and α values. (*B*) FWHM evolution profiles of 2-μm particles from $Re_p = 0.0025$–0.0125 (dot sign) and 1-μm particles at $Re_p = 0.0031$ (plus sign). (*C*) Images of the microchannel ($L = 2$ cm, $H = 80$ μm) before and after focusing bacteria (0.8 μm) *S. aureus*. (*D*) Attained focus lengths of 1- and 2-μm particles and bacteria at varying Re_p (*a shorter device is used for the bacteria experiments to achieve higher Re_p).

Dimensionless Parameter α. We demonstrated that the inertial focusing at low Re_p is not only limited by the required focus lengths and pressures but also by the diffusion rate of small particles' being significant compared with their inertial migration velocity. Theoretically, this limitation was evaluated by calculating an inertial migration equivalent to the Peclet number, defined as the ratio of the inertial migration velocity of the particle under flow (U_P) to the diffusion coefficient of the particle (D) for a given characteristic length (L_c) as

$$\alpha = L_C(U_p/D). \quad [3]$$

α is a measure of the relative magnitudes of the two major phenomena that determine the migration of the particle at very low Re_p flows: inertial migration and diffusion. A natural choice for L_c is the channel dimension along particle migration and was selected as half of that dimension ($H/2$) due to symmetry. Assuming a spherical shape, the diffusion rate of the particle is correlated to its size by the Stokes–Einstein equation $D = k_BT/3\pi\mu a$, where k_B is the Boltzmann constant and T is the temperature. Thus, we can insert the expressions for both inertial migration velocity and diffusion into α to obtain

$$\alpha = \frac{H}{2}\cdot\frac{U_p}{D} = \frac{Ha3\pi\mu}{2k_BT}\cdot U_p = \frac{Ha3\pi\mu}{2k_BT}\cdot\frac{f_L\rho {U_m}^2 a^3}{3\pi\mu H^2} = \frac{a^4 f_L \rho {U_m}^2}{2k_BTH} = \frac{\rho}{2k_BT}\cdot\frac{f_L}{H}\cdot a^4\cdot {U_m}^2. \quad [4]$$

Eq. **4** provides an important insight to an inherent physical limitation that arises when inertially focusing particles at very low Re_p flows. α is a quartic function of the particle size (a) but only a quadratic function of the flow velocity (U_m). Conventionally, diffusion is not considered in inertial microfluidics, because the diffusion rate of particles is considered negligible in the typical Re_p (>0.1) ranges. This can be verified by further analysis of the terms of Eq. **4** to reveal an intrinsic relationship between α and Re_p [$= \rho U_m a^2(\mu D_h)^{-1}$] as

$$\alpha = \frac{f_L\mu^2}{2k_BT\rho}\cdot\left(\frac{D_h^2}{H}\right)\cdot(Re_p)^2 = C\cdot f_L\cdot\left(\frac{D_h^2}{H}\right)\cdot(Re_p)^2 \approx C\cdot f_L\cdot D_{ch}\cdot(Re_p)^2. \quad [5]$$

In Eq. **5**, the first term (C) has the dimensions of [1/length] and encompasses the parameters that are constant when the working fluid and the temperature of the system are fixed. The second term contains only the dimensions (${D_h}^2/H$) of the channel and can be further approximated if the cross-sectional dimensions of the channel are comparable (i.e., a square channel). In that case, the second term reduces to a length-scale term: $D_{ch} \approx H \approx D_h$. Thus, for a preset working fluid and a microfluidic channel at a given temperature, α becomes a quadratic function of Re_p. Assuming properties of water at room temperature, the value of C can be evaluated as 123.5×10^9 m^{-1}. Using some typical microchannel dimensions ($H = 50$ μm, $f_L = 0.04$), for $Re_p = 0.1$–1, α is on the order of 10^3 to 10^5. Since α is a measure of particle's inertial migration velocity to its diffusion, for such large values of α (when $Re_p > 0.1$), it is reasonable to expect that diffusion is negligible. It is only when Re_p is further decreased to the order of 10^{-2}, where α reduces to the order of 10, that diffusion becomes nonnegligible.

At the minimum Re_p (0.0025) where no focusing was observed, the α value was below unity: $\alpha = 0.88$. At $Re_p = 0.0031$–0.0050, a range where a decrease in focus quality was observed, α ranged from 1.39 to 3.55 (using bacteria and 1- to 2-μm particles). As α became significantly larger than unity, focus quality improved, but not drastically beyond $\alpha = 7.98$. Based on these results, we concluded that $\alpha >> 1$ is required for the diffusion effects to be negligible in inertial microfluidic systems. Presenting the experimental

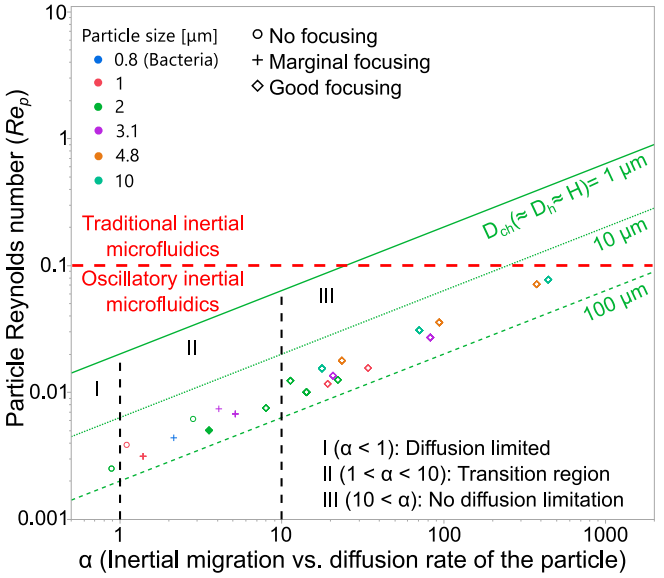

Fig. 5. Dimensionless parameter space explored in this study.

data in an α vs. Re_p plot reveals distinct regimes of microfluidic inertial focusing (Fig. 5). Traditional, steady-flow inertial microfluidics has been limited due to the impractical focusing lengths and driving pressures required at very low Re_p values. Thus, $Re_p \approx 0.1$ has been a natural lower boundary in the field. Note that for typical length scales of microfluidic channels, diffusion of particles is negligible at $Re_p > 10^{-1}$, because the corresponding α values are much greater than unity. However, in the oscillatory inertial microfluidics region explored in this study, our experimental data lie between $0.002 < Re_p < 0.1$ and $0.8 < \alpha < 500$. Thus, as α was decreased, we observed the system transition from negligible diffusion and good focusing to reduced focus quality, and eventually to no inertial focusing behavior. Based on these observations, these three regions were identified as (*i*) diffusion limited, (*ii*) transition, and (*iii*) no diffusion limitation.

The α value can be determined without making any assumptions about the system (using Eq. **3**), if the migration velocity of the particles and the particle diffusion coefficient are measured or otherwise known. In this study, the characteristic length L_c is selected as half of the channel dimension where inertial migration is observed; however it could be replaced by the desired width of the focus stream, if known. However, for practical purposes, Eqs. **4** and **5** provide a rapid nondimensional tool for characterizing the diffusion limitations in a microfluidic system. Many microfluidic devices run at room temperature with water-based fluids, and thus simply by knowing the characteristic dimension of the channel (D_{ch}) and Re_p one can determine the impact of diffusion on the inertial focusing performance of the system. While outside the scope of this study, the limitations of the assumptions leading to Eq. **5**, and the extension of it to curved channels utilizing Dean flow, need to be explored.

Varying Cross-Section (Dog-Bone) Microchip Design. Based on our findings, we developed a prototype dog-bone-shaped microfluidic chip for inertially focusing smaller (i.e. a few hundreds of nanometers) particles. Our previous results demonstrated that to achieve high-quality inertial focusing, Re_p and α need to be sufficiently high (Fig. 5). Thus, the further decrease in the particle size needs to be compensated by increased flow velocity. To achieve this, a varying-cross-section microchip was designed with a very narrow and short section, where the small cross-sectional area and short length enables higher flow velocity. The narrow section is connected to two wider sections of the channel, where the pressure drop is reduced, and the decreased flow velocity ensures that the particles are kept in the channel during their oscillation. The resulting shape, similar to a dog bone, is shown in Fig. 6.

It was observed that at $P = 25$ psi, 500-nm particles focused on the side-focusing positions of the channel (Fig. 6 and Movie S4), as a result of the preferred focusing positions shifting to the sides due to the high depth-to-width ratio ($W/H = 6.4$) of the narrow section. Even though this ratio is less than unity in the expansion section ($W/H = 0.42$), the inertial lift forces are also significantly weaker, and thus the focusing positions are determined by the geometry of the narrow section where focusing takes place. Using this geometry, the corresponding flow parameters in the narrow section of the channel were calculated as $Re_p = 0.052$ and $\alpha = 400$, well within the range where we were able to obtain focusing using straight channels (Fig. 5). Similar to those results, focusing was attained in a short time scale ($t_f = 10$ s).

Shear Stress at Very Low Re_p. Operating at a very low Re_p range also enables particles that are similar to WBCs in size (10 μm) to be inertially focused at very low input pressures and larger channels, which translates to cells being exposed to minimal, physiological-scale shear-stress levels. This is desirable to ensure that cells remain unharmed and do not exhibit a shear-induced response, and also to avoid clogging and malfunction of blood processing devices, due to shear stress activation of platelets and von Willebrand factor fibers (26, 27). The physiological shear stress levels in the veins and arteries are reported as 1–6 dynes/cm^2 and 10–70 dynes/cm^2, respectively (28). We conducted a finite element simulation of a fully developed flow in our microchannel (*SI Appendix*, Fig. S5) and evaluated the maximum (on the channel wall) and the average shear stress as 18.4 dynes/cm^2 and 8.3 dynes/cm^2, respectively.

System Throughput. In an oscillatory inertial microfluidics system, the physical length of the channel is shorter (with respect to traditional steady flow) and is virtually extended by making the particles spend more time in the channel. This, in return, reduces the throughput per channel proportionally with the extended time. For instance, if the inertial focusing length is extended an order of magnitude via oscillatory flow, it is expected that the throughput of the system will decrease an order of magnitude, if no other changes are made to the system.

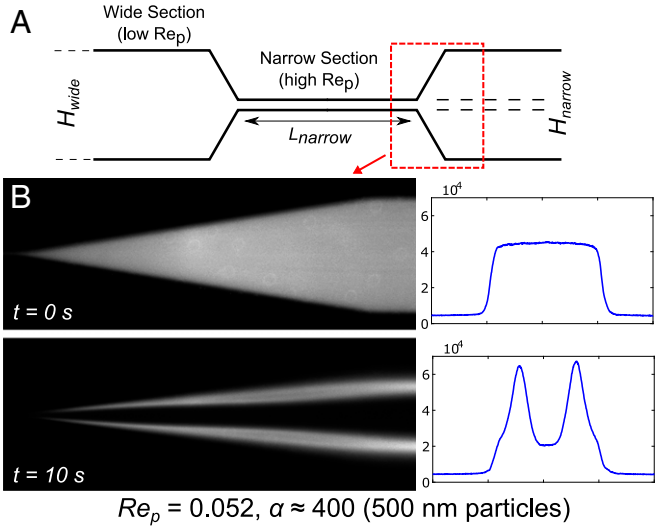

Fig. 6. Oscillatory inertial focusing of 500-nm particles using a dog-bone-shaped microchannel. (*A*) Schematic of the microchannel (H_{narrow} = 10 μm, L_{narrow} = 250 μm, H_{wide} = 150 μm, L_{wide} = 5.5 cm, and W = 64 μm). (*B*) Oscillatory inertial focusing with 500-nm particles. Fluorescent streak images (*Left*) and FWHM profiles (*Right*) show the focusing of particles.

We propose that this reduction in the single-channel throughput can be alleviated by increased parallelization of the channels. Due to the shorter channel length, it would be possible to fit more devices in the same overall footprint, which enhances parallelization and scaling. For instance, if the inertial focusing length is extended 10-fold via oscillatory flow, 10 times the number of channels could be fitted in the same geometry instead of an equivalent, 10-fold longer channel. In addition, in the oscillatory case, the pressure drop would be significantly less due to the shorter channel length. It should be noted that while the higher parallelization would bring additional engineering design challenges, the feasibility of highly parallelized microfluidic chips on injection-molded plastic devices has been successfully demonstrated (29).

Conclusion

In summary, oscillatory inertial microfluidics achieves inertial particle manipulation and focusing in a previously inaccessible flow regime, specifically at a very low Re_p range ($Re_p < 0.01$) and particle-to-channel ratios ($a/H < 0.1$). We demonstrated this by inertially focusing a variety of particles—as small as 500 nm—in oscillatory flows, including a bacterium (*S. aureus*) in an 80-μm-wide microchannel using 20 psi driving pressure, which corresponded to $Re_p = 0.0047$ and $a/H = 0.01$. After demonstration of the method, we described the key principles for the design and operation of microfluidic devices at this flow regime, based on experimental observations and a nondimensional analysis of inertial migration and self-diffusion rate of particles.

The developed system can enable a new generation of inertial microfluidic devices which are unfeasible to implement using traditional, steady-flow microfluidics. While an analytical system was used in this study to be able to investigate a wide range of parameters (in terms of particle size, particle-to-channel ratio, and the dimensionless parameters Re_p and α), purpose-built systems would be required to evaluate the performance of the proposed method for specific applications. These applications include inertial manipulation of smaller bioparticles such as bacteria, for the development of isolation devices based on label-free sorting of the pathogens. Larger bioparticles such as nucleated cells (e.g., CTCs and WBCs) can be sorted at physiological shear stresses to ensure that the cells do not get damaged or exhibit any flow-induced response, and also be repeatedly imaged on their focus plane while rotating for biophysical characterization or high-sensitivity flow cytometry applications. We also expect that the very low particle-to-channel ratio can potentially extend the capabilities of inertial microfluidics to allow the use of easy-to-manufacture, millimeter-scale devices (e.g. manufactured via 3D printing) for cell and bioparticle processing.

Materials and Methods

Monodisperse fluorescent polystyrene particles (Fluoro-Max; Sigma Aldrich) and bacteria (SH1000-GFP *S. aureus* strain, which expresses green fluorescent protein) were diluted in PBS solutions and density-matched by adding Optiprep (Sigma-Aldrich). Stock solutions of particles were received at 1% wt/vol concentration, and their final concentration (after dilution) ranged from 0.02 to 0.001% wt/vol based on the particle size. Bacteria were harvested at 1.7×10^9 cells per mL concentration and diluted 100-fold before being used in the experiments. An air compressor which can deliver up to 25 psi pressure was used to drive the flow. The high-speed three-way solenoid valves (LHDA0533315H) were obtained from The Lee Company. PDMS devices were fabricated using standard soft lithography techniques (30). Microfluidic devices used with larger (a = 3-, 4.8-, and 10-μm) particles had a width (H) of 80 μm and a length (L) of 4.3 cm, devices used with smaller (a = 1 or 2 μm) particles had H = 40 μm and L = 6.2 cm, and the device used with bacteria (a = 0.8 μm) had H = 80 μm and L = 2 cm. The prototype dog-bone microfluidic device had a narrow section with H = 10 μm and L = 250 μm and an expansion section with H = 150 μm and L = 5.5 cm. All channels had a fixed depth, $W = 25 \pm 3$ μm, except for the dog-bone device which had $W = 64 \pm 2$ μm. The components of the system were connected to each other via Tygon tubing (Cole Parmer). A monochrome Retiga 2000R camera (QImaging) was used to record streak images of the particles. Inertial migration video of an individual particle (Movie S1) was obtained by recording with a high-speed camera (Phantom 4.2; Vision Research Inc.) at a frame capture rate (10 frames per s) that matches the oscillation frequency of the flow (10 Hz). Therefore, the particle appears to have very minimal horizontal movement, despite traveling outside the field of view and coming back in an oscillation cycle.

ACKNOWLEDGMENTS. We thank O. Hurtado for his help with microfabrication, and C. Dietsche for helpful discussions. This work was partially supported by National Institute of Biomedical Imaging and Bioengineering BioMEMS Resource Center Grant P41 EB002503.

1. Di Carlo D, Irimia D, Tompkins RG, Toner M (2007) Continuous inertial focusing, ordering, and separation of particles in microchannels. *Proc Natl Acad Sci USA* 104: 18892–18897.
2. Segré G, Silberberg A (1961) Radial particle displacements in Poiseuille flow of suspensions. *Nature* 189:209–210.
3. Di Carlo D, Edd JF, Irimia D, Tompkins RG, Toner M (2008) Equilibrium separation and filtration of particles using differential inertial focusing. *Anal Chem* 80:2204–2211.
4. Lee WC, et al. (2011) High-throughput cell cycle synchronization using inertial forces in spiral microchannels. *Lab Chip* 11:1359–1367.
5. Hou HW, et al. (2013) Isolation and retrieval of circulating tumor cells using centrifugal forces. *Sci Rep* 3:1259.
6. Sollier E, et al. (2014) Size-selective collection of circulating tumor cells using Vortex technology. *Lab Chip* 14:63–77.
7. Gossett DR, et al. (2012) Hydrodynamic stretching of single cells for large population mechanical phenotyping. *Proc Natl Acad Sci USA* 109:7630–7635.
8. Ozkumur E, et al. (2013) Inertial focusing for tumor antigen-dependent and -independent sorting of rare circulating tumor cells. *Sci Transl Med* 5:179ra47.
9. Martel JM, et al. (2015) Continuous flow microfluidic bioparticle concentrator. *Sci Rep* 5:11300.
10. Warkiani ME, et al. (2016) Ultra-fast, label-free isolation of circulating tumor cells from blood using spiral microfluidics. *Nat Protoc* 11:134–148.
11. Miller B, Jimenez M, Bridle H (2016) Cascading and parallelising curvilinear inertial focusing systems for high volume, wide size distribution, separation and concentration of particles. *Sci Rep* 6:36386.
12. Hur SC, Tse HTK, Di Carlo D (2010) Sheathless inertial cell ordering for extreme throughput flow cytometry. *Lab Chip* 10:274–280.
13. Gossett DR, et al. (2012) Inertial manipulation and transfer of microparticles across laminar fluid streams. *Small* 8:2757–2764.
14. Mutlu BR, et al. (2017) Non-equilibrium inertial separation array for high-throughput, large-volume blood fractionation. *Sci Rep* 7:9915.
15. Martel JM, Toner M (2014) Inertial focusing in microfluidics. *Annu Rev Biomed Eng* 16: 371–396.
16. Angus DC, van der Poll T (2013) Severe sepsis and septic shock. *N Engl J Med* 369: 840–851.
17. Skog J, et al. (2008) Glioblastoma microvesicles transport RNA and proteins that promote tumour growth and provide diagnostic biomarkers. *Nat Cell Biol* 10: 1470–1476.
18. Melo SA, et al. (2015) Glypican-1 identifies cancer exosomes and detects early pancreatic cancer. *Nature* 523:177–182.
19. Mach AJ, Di Carlo D (2010) Continuous scalable blood filtration device using inertial microfluidics. *Biotechnol Bioeng* 107:302–311.
20. Warkiani ME, et al. (2015) Malaria detection using inertial microfluidics. *Lab Chip* 15: 1101–1109.
21. Matas JP, Morris JF, Guazzelli É (2004) Inertial migration of rigid spherical particles in Poiseuille flow. *J Fluid Mech* 515:171–195.
22. Asmolov ES (1999) The inertial lift on a spherical particle in a plane Poiseuille flow at large channel Reynolds number. *J Fluid Mech* 381:63–87.
23. Di Carlo D (2009) Inertial microfluidics. *Lab Chip* 9:3038–3046.
24. Di Carlo D, Edd JF, Humphry KJ, Stone HA, Toner M (2009) Particle segregation and dynamics in confined flows. *Phys Rev Lett* 102:094503.
25. Amini H, Lee W, Di Carlo D (2014) Inertial microfluidic physics. *Lab Chip* 14:2739–2761.
26. Schneider SW, et al. (2007) Shear-induced unfolding triggers adhesion of von Willebrand factor fibers. *Proc Natl Acad Sci USA* 104:7899–7903.
27. Ramstack JM, Zuckerman L, Mockros LF (1979) Shear-induced activation of platelets. *J Biomech* 12:113–125.
28. Malek AM, Alper SL, Izumo S (1999) Hemodynamic shear stress and its role in atherosclerosis. *JAMA* 282:2035–2042.
29. Fachin F, et al. (2017) Monolithic chip for high-throughput blood cell depletion to sort rare circulating tumor cells. *Sci Rep* 7:10936.
30. Duffy DC, McDonald JC, Schueller OJA, Whitesides GM (1998) Rapid prototyping of microfluidic systems in poly(dimethylsiloxane). *Anal Chem* 70:4974–4984.